Pressure drops prediction in gas–liquid mixtures flowing upflow in vertical ducts

C. Lombardi, A. Cammi*, E. Faimali

Politecnico di Milano, Department of Energy, CeSNEF (Enrico Fermi Center for Nuclear Studies), via Ponzio 34/3, 20133 Milano, Italy

Article history:
Received 19 April 2013
Received in revised form
21 October 2013
Accepted 10 November 2013

1. Introduction

According to the relevant literature of pressure drops in two phase flow, the total pressure drop expression is usually subdivided in the same three terms, which are used in single phase approach: gravitational, kinetic or acceleration, and friction terms. In a single phase flow, the main goal of this subdivision is to make the empirical correlations for the friction pressure drops, independent from the duct inclination (Collier and Thome, 1996), rather than the exact calculation of the single terms (which are not directly measurable without using some very specific procedures). On the contrary, in two phase flow, the friction of pressure drops depends significantly on the duct inclination, thus requiring a specific empirical correlation for each inclination (Collier and Thome, 1996). Therefore, in two phase flow, this approach does not seem to be advantageous, though widely used and we shall adopt this same method.

In two phase flow, there are some differences between deriving pressure drops breakdown from either the momentum or the energy balance, while this issue does not arise with a single phase flow, where equivalence was demonstrated between the two balances (Bennett and Myers, 1974). In literature, almost all the two phase correlations are derived by the momentum balance approach, while on the contrary, all Cesnef correlations, developed in this Department, were obtained by the energy balance one.

In the energy balance approach, gravitational pressure drop is proportional to a mixture density, equal to the known flow rate density, which is mathematically identical to the homogeneous mixture density. On the contrary, the momentum balance requires the knowledge of the actual density inside the channel, which can be determined only by complex and not well known empirical correlation. The homogeneous value may be adopted, but this is only an approximation; its validity depends on the flow parameters: for instance high mass fluxes and high pressures better approach this assumption (the discussion is detailed in Section 2).

In the past, one of the authors contributed to the development of different versions of a pressure drop correlation for two phase mixtures, the most recent of them are named Cesnef-2 (Lombardi and Carsana, 1992) and Cesnef-3 (Lombardi et al., 2000). In most applications they show similar predictive capabilities; Cesnef-3 is applicable also to high density fluids (liquid lead or lead bismuth) and to near critical conditions of the fluid, but it loses partially its dimensionless form, which is well verified in Cesnef-2. They are detailed in Table 1.

Let us recall their common features:

- they use a breakdown of the total pressure drops, according to both the energy balance and the homogeneous model (see Section 2), where only the friction pressure drop is empirically correlated;

* Corresponding author.
E-mail address: antonio.cammi@polimi.it (A. Cammi).

Table 1
CESNEF-2 and CESNEF-3 correlations.

Total pressure drop	The total pressure drop dP in an infinitesimal length dh is given by: $dp = dp_f + dp_h + dp_k$ where: $dp_f = \frac{2f}{D} G_m^2 v_m dh$ (friction term) $dp_h = \frac{1}{v_m} g dh$(head term) $dp_k = G_m^2 dv_m$ (kinetic term) Note: when $Lo < k_m\, Ce$, dp cannot be higher than liquid column weight, i.e. $\rho_l\, g\, dh$.	
Friction term	$\boldsymbol{f = f_g b_g + f_l b_l + f_m b_m}$ $\boldsymbol{f_g}$ and $\boldsymbol{f_l}$ are the single-phase friction factors, calculated at the same total mass flux $\boldsymbol{G_m}$; $\boldsymbol{b_g}$ and $\boldsymbol{b_l}$ are weight functions; $\boldsymbol{f_m}$ is the mixture friction factor with its respective weight $\boldsymbol{b_m}$	
Single phase friction term	$\boldsymbol{f_{g/l} = \left[3.8 log\left(\frac{10}{Re_{g/l}} + 0.2\frac{e}{D}\right)\right]^{-2}}$ $\boldsymbol{f_{g/l} = \frac{16}{Re_{g/l}}}$	Re $\geq$ 2400 Re $<$ 2400
Mixture friction term	$\boldsymbol{f_m = k_1 (Lo)^{-0.25}}$ $\boldsymbol{f_m = k_1 (k_2 Ce)(Lo)^{-1.25}}$	$\boldsymbol{Lo \geq k_2 Ce}$ $\boldsymbol{Lo < k_2 Ce}$
Dimensionless numbers	$\boldsymbol{Lo = \frac{G_m^2 v_m D}{\sigma}\left(\frac{\mu_g}{\mu_l}\right)^{0.5}}$ where $\boldsymbol{v_m = x v_g + (1-x) v_l}$	$\begin{cases} Ce = \rho_l g \frac{(D-D_0)^2}{\sigma}\frac{\mu_g}{\mu_l}, & D > D_0 \\ Ce = 0, & D \leq D_0 \end{cases}$ $D_0 = 0.001\ m$
Cesnef-2		Cesnef-3
$k_1 = 0.046$ $k_2 = 30$		$k_1 = 0.044$ $\boldsymbol{k_2(\rho_l) = 31.5\left(\frac{\rho_L}{\rho_{L0}}\right) - 1.5\left(\frac{\rho_L}{\rho_{L0}}\right)^2}$ $\boldsymbol{\rho_{L0} = 1000\ kg\ m^{-3}}$
$\boldsymbol{b_g = x^{600\left(v_l/v_g\right)}}$ $\boldsymbol{b_l = (1-x)^{2\left(v_g/v_l\right)}}$ $\boldsymbol{b_m = 1 - b_g - b_l}$		$b_g = (x_v)^{m_g}$ $b_l = (1-x_v)^{m_l}$ $b_m = 1 - b_g - b_l$ $\boldsymbol{m_{g/l} = \left[ln\left(e - 1 + \frac{v_g}{v_l}\right)\right]^{k_{gl}}}$ $k_l = 0.5$; $k_g = 3.3$

- there is a continuous and smooth transition between single-phase and two phase pressure drops trends, as found experimentally;
- they can be applied both to adiabatic and diabatic conditions and they are verified in a wide range of parameters, including very low mass fluxes and large diameters;
- good reliability in their field of validity;
- a remarkable analogy with single phase correlations can be demonstrated, by replacing Reynolds number with the new dimensionless Lo number;
- for mass flux coming closer to zero, they would give an infinite value for the total pressure drop, but this is avoided by imposing a physical limit, equal to the weight of the liquid column, which is supposed to fill the whole channel in these conditions;
- by reducing the Lo number, i.e. by reducing the mass flux or increasing the diameter or the liquid density, they present, at a given point ($Lo = k_2\, Ce$), a sudden change in friction pressure drop trend, probably due to a drastic change in the phase distribution;
- most of the data are in the zone $Lo \geq k_2\ Ce$, i.e. above the transition;
- for capillary tubes (diameter less than 0.001 m) the transition for $Lo = k_2\, Ce$ is not experimentally verified and then eliminated by a suitable definition of the Ce number; from a physical point of view, it seems correct to imagine that in a very small tube the border effects can become important, in order to avoid the sudden change in friction pressure losses.

On the other hand, the two correlations show some differences:

- the weight functions b_g and b_l take into account the increasing importance of single phase pressure drops when the fraction of each phase approaches the unity. Therefore, in both correlations, they obey the following limits, although by different expressions:

$$\text{gas fraction} \to 0 \quad b_l \to 1,\ b_g \to 0,\ b_m \to 0 \tag{1}$$

$$\text{gas fraction} \to 1 \quad b_l \to 0,\ b_g \to 1,\ b_m \to 0 \tag{2}$$

$$0 < \text{gas fraction} < 1 \quad b_m = 1 - b_l - b_g \tag{3}$$

But in Cesnef-3, a further limit is imposed to take into account that at the critical pressure the two phases are identical and the fluid behaves as in single phase flow, then:

$$\text{for any gas fraction and } p \to p_{cr} \quad (b_l + b_g) \to 1, b_m \to 0 \tag{4}$$

- experimental data relevant to a very peculiar mixture made by liquid eutectic lead-bismuth (density about 10 times the water one), require a substantial increase of the constant k_2 from 30 to 430; then Cesnef-2 is inapplicable to these high density mixtures. It is worth noting that the experimental evidence is rather meagre (only one situation) and that the friction losses are much lower than the head term, although calculated with the homogeneous model. For their prediction, Cesnef-3 uses a different function for k_2, which makes this term no longer dimensionless. In fact, the adoption of the ratio of the true liquid density over ambient water density, is only a normalization process, without any physical meaning; the remaining part of the correlation is the same, apart from a modest reduction of k_1 from 0.046 to 0.044.

Table 2
Error statistics for pressure drop predictions by CESNEF-2 and CESNEF-3 correlations.

			N° exp	D (mm)	G (kg m^{-2} s^{-1})	p (kPa)	Cesnef-2			Cesnef-3		
				min/max	min/max	min/max	AE (%)	RMS (%)	±20%	AE (%)	RMS (%)	±20%
M	T	A	1949	5/25	333/4398	1962/9642	8.93	16.58	79.04	4.55	16.82	79.38
		D	6708	4/25	44/5172	134/19967	11.14	22.31	68.69	8.32	21.88	69.77
	C	A	369	5/12	221/4577	3024/7256	−2.63	12.89	90.51	−7.62	15.18	80.49
		D	3804	3/25	76/4581	1033/8904	8.18	25.10	71.79	5.70	24.77	70.43
B	T		2339	9/446	20/3420	101/2383	2.70	14.67	86.67	−5.38	19.9	80.68
	C		333	7/15	50/2880	205/2137	3.18	10.62	92.19	−7.46	15.05	80.48
B	Cap		99	0.5/2	3/122	101	20.3	37.02	29.29	26.64	39.93	19.19
	ALC		553	7/25	57	176/2137	17.09	35.30	48.28	5.70	32.32	45.93
ALL			16,154	0.5/446	3/5172	101/19967	8.86	21.82	73.31	4.60	22.14	68.66
Pb−Bi/steam			79	203	6211/14122	541/687	N.A	N.A	N.A	−6.40	6.87	100

M − monocomponent; B − bicomponent; T − tubular; C − complex geometry; A − adiabatic; D − diabatic; Cap − capillary; ALC − alcohol data.

The statistics analysis of the predictions of Cesnef 2 and Cesnef 3 for a large amount of data (Lombardi et al., 2000), are reported in Table 2. The predictions are really satisfactory and the two correlations appear almost equivalent, except for Pb−Bi/steam mixture, as above explained.

The Cesnef-2 was also applied to very deep geothermal wells, to predict pressure and temperature profiles along the length (up to about 1400 m) of steam−water mixtures, yielding good results for pressure profiles and less satisfactory results, although still acceptable, for the temperature profiles (Barelli et al., 1994). Possible explanations are:

- these in field data are less accurate than laboratory data;
- an unpredictable in service modification of the inside surface;
- uncertainties in heat losses along the well and among different wells;
- the not complete validity of the hypotheses used in the calculations (the Dalton and Henry laws, the thermodynamic equilibrium and the value of Henry constant).

However, in the reference, it was suggested that the k_2 value should be slightly lowered from 30, and this is obtained in Cesnef 3, which gives about 27, with modest variations along the length, according to the change of fluid parameters versus temperature. This behaviour stands in favour of Cesnef 3, although not substantial.

All the above taken into account, it was decided to reconsider all the work done in the past for pressure drop prediction in two phase flow, with specific reference to Cesnef correlations development, with the aim to:

- detail the difference between the momentum and the energy balance approaches (Section 2);
- check the coherence between experimental data obtained in adiabatic and diabatic conditions, to better justify the adoption of the same correlation to predict both these data (Section 3);
- revise the Cesnef-3 correlation in the $Lo < k_2$ Ce zone, trying to simplify it (Section 4); even though this zone is seldom obtained in practical applications, it is interesting for its physical implications at very low flow rates or high diameters;
- compare the reliability of Cesnef correlations with respect to other well-known correlations (Section 5).

2. Energy and momentum approaches in deriving two phase total pressure drop breakdown

The two phase-pressure drops between two sections of a duct can be ideally subdivided in the same three terms already defined in single phase flow: *gravitational*, *kinetic or acceleration*, *dissipative or friction*.

Applying the energy balance to a duct portion dz, inclined of an angle γ with respect to the vertical direction, crossed by gas and liquid mass flow rates Γ_g and Γ_l, with the addition of thermal energy dW_t, the following equation is obtained:

$$d(\Gamma_g U_g) + d(\Gamma_l U_l) + \Gamma_g g\cos\gamma dz + \Gamma_l g\cos\gamma dz + d(\Gamma_g e_g) + d(\Gamma_l e_l) + d(\Gamma_g p v_g) + d(\Gamma_l p v_l) - dW_t = 0 \quad (5)$$

where U and e are the internal energy and the kinetic energy per unit mass of both phases respectively, g the gravity constant, p the pressure, v the specific volume. Dividing this equation by the total flow rate, the following equation is obtained:

$$d\left[xU_g + (1-x)U_l\right] + g\cos\gamma dz + d\left[xe_g + (1-x)e_l\right] + d\left\{p\left[xv_g + (1-x)v_l\right]\right\} - \frac{dW_t}{\Gamma} = 0 \quad (6)$$

where x is the gas mass fraction.

Defining the mixture parameters with the index m, averaged by the relative mass fraction, the following equation can be obtained:

$$dU_m + g\cos\gamma dz + de_m + d(pv_m) - dW_t/\Gamma = 0 \quad (7)$$

which is formally identical to the single phase energy balance. Introducing the following terms:

$$\rho_m = \frac{1}{v_m} = \frac{1}{xv_g + (1-x)v_l} \quad (8)$$

$$dR_m = dU_m + p dv_m - dW_t/\Gamma \quad (9)$$

analogously to single phase situation it is obtained:

$$dR_m = dU_m + p dv_m - dW_t/\Gamma \quad (10)$$

$$-dp = dp_h + dp_k + dp_f \tag{11}$$

where:

$$\text{gravitational term} \quad dp_h = \rho_m g \cos\gamma dz \tag{12}$$

$$\text{kinetic term} \quad dp_k = \rho_m de_m \tag{13}$$

$$\text{dissipative or friction term} \quad dp_f = \rho_m dR_m \tag{14}$$

ρ_m and v_m represent *the flow rate density* and *the flow rate specific volume* respectively (mathematically equal to the homogeneous values); they have not a precise correspondence to what occurs inside the channel, being in general different from actual values: there is a coincidence only in the case of a perfect homogeneous mixture (average slip ratio equal to 1).

The kinetic term, which represents the mixture kinetic energy variation along the duct axis, is very difficult to calculate; the analytical expression is:

$$dp_k = \rho_m de_m = \rho_m d\left[xe_g + (1-x)e_l\right] = \rho_m d\left[\frac{x}{2} a_g \overline{u}_g^2 + \frac{1-x}{2} a_l \overline{u}_l^2\right] = \rho_m d\left[\frac{x}{2} a_g \frac{I^2 x^2 v_g^2}{\overline{\alpha}^2 \Omega^2} + \frac{1-x}{2} a_l \frac{I^2 (1-x)^2 v_l^2}{(1-\overline{\alpha})^2 \Omega^2}\right] \tag{15}$$

where a_g and a_l are the two phase Coriolis coefficients and Ω the duct cross section:

$$a_g = \frac{\int_\Omega u_g^3 d\Omega_g}{\overline{u}_g^3 \Omega_g} \tag{16}$$

and analogously for a_l.

Accepting this breakdown, there are various alternative solutions to overcome the computation difficulties:

a) empirically correlate together ($dp_k + dp_f$);
b) calculate dp_k recurring to other correlations for the needed parameters;
c) calculate dp_k by the homogeneous model, considering that the difference with the true value (the error) can be lumped together in dp_f, i.e. inherently taken into account when correlating it.

The three solutions are completely equivalent, provided that the same route is followed when predicting the total pressure drops.

The available correlations in the relevant literature are almost always referred to a momentum balance, which, otherwise single phase flow, yields in this case rather different formulations. In the momentum balance approach Eq. (11) remains the same, but the three terms are:

$$\text{gravitational term} \quad dp_h = \rho_{m,act}\, g \cos\gamma dz \tag{17}$$

$$\text{acceleration term} \quad dp_a = dM_m/\Omega \tag{18}$$

$$\text{friction term} \quad dp_f = 4(\tau/D_e)d_z \tag{19}$$

where $\rho_{m,act}$ is the actual mixture density, M_m the momentum and τ the wall shear stress and D_e the equivalent diameter. The acceleration term is equal to:

$$dp_a = d\left[\rho_g \overline{u}_g^2 \beta_g \overline{\alpha} + \rho_l \overline{u}_l^2 \beta_l (1-\overline{\alpha})\right] \tag{20}$$

where β_g and β_l:

$$\beta_g = \frac{\int_\Omega u_g^2 d\Omega_g}{\overline{u}_g^2 \Omega_g} \tag{21}$$

and analogously for β_l.

In this case, not only there are, for the momentum variation, the same difficulties encountered for kinetic energy variation, but also dp_h cannot be directly calculated by the system parameters. Considering also that the energy formulation remains the same for ducts of non-uniform cross section, we think of that it is to be preferred to the momentum balance one. In conclusion, both approaches require an empirical correlation for the friction term, but the momentum one requires an empirical correlation also for the mixture density, while the energy one correctly uses the calculated value given by the homogeneous approach. The mixture density correlations are generally given for specific conditions, then their reliability is questionable: no general correlation is available in the literature. For the acceleration term and the corresponding kinetic term, both approaches are in trouble, since for their correct definition velocity and phase distributions along any cross section are needed and this is a complex and unsolvable problem: in adiabatic conditions these terms are in general small and then the difficulty can be faced by calculating them by the assumption of the homogeneous hypothesis (as done above), but in diabatic conditions this is no longer true and a solution is to be found: above it is said that in our correlation, the error done by the homogeneous assumption is ideally transferred in the empirical correlation of the friction term, but its validity is to be verified by experimental evidence. Then in our opinion, the energy approach, facilitates the correlating effort of total pressure drops. However, we are well aware that in non-steady conditions both formulations are needed. In our case we have adopted the above solution c), i.e. the homogeneous model for calculating the kinetic term.

In a rather old work (Lombardi and Terlizzi, 1992), with the participation by one of the authors, it was shown that by applying either the energy balance or the momentum one, the resulting experimental friction pressure drops can be significantly different. Let us here recall the synthesis. The MIDA bank (Brega et al., 1990),

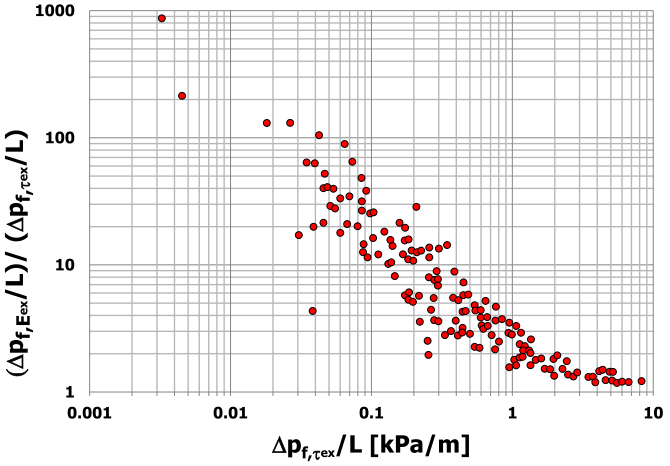

Fig. 1. Reproduction of Fig. 1 of (Lombardi and Terlizzi, 1992) – experimental friction pressure drop ratio according to energy and momentum balance versus friction pressure drop according to momentum balance.

widely used in this work, contains 283 experimental situations relevant to eight different geometries or type of mixtures, always in adiabatic conditions, in which pressure drops and whole channel densities are measured at the same time. These data allow us to define two different friction terms (E for energy, M for momentum) and namely:

$$\left(\frac{\Delta p}{L}\right)^{E}_{\boldsymbol{f,exp}} = \left(\frac{\Delta p}{L}\right)_{\exp} - \left(\frac{\Delta p}{L}\right)^{E}_{\boldsymbol{h}} - \left(\frac{\Delta p}{L}\right)_{k} = \left(\frac{\Delta p}{L}\right)_{\exp} - \rho_m g - \frac{G_m^2}{L}\left(\frac{1}{\rho_{m,\text{out}}} - \frac{1}{\rho_{m,\text{in}}}\right) \quad (22)$$

$$\left(\frac{\Delta p}{L}\right)^{M}_{f,\exp} = \left(\frac{\Delta p}{L}\right)_{\exp} - \left(\frac{\Delta p}{L}\right)^{M}_{h} - \left(\frac{\Delta p}{L}\right)_{a} = \left(\frac{\Delta p}{L}\right)_{\exp} - \rho_{m,\text{act}} g - \frac{G_m^2}{L}\left(\frac{1}{\rho_{m,\text{out}}} - \frac{1}{\rho_{m,\text{in}}}\right) \quad (23)$$

where G_m is the mass flux, L is the duct length, the subscripts f and exp are referred to the friction term and the experimental data, respectively. The kinetic term (energy) and the acceleration term (momentum) have here the same value, being calculated by adopting the homogeneous hypothesis, which is well justified in these adiabatic conditions, where these terms are relatively very small. The density used for the gravitational term is the average value between inlet and outlet conditions. The ratio between the two definitions goes from about one thousand to one by increasing the term $(\Delta p/L)^{M}_{f,\exp}$: see Fig. 1 taken from the original one (Lombardi and Terlizzi, 1992) and Table 3, detailing the same data.

3. Coherence between adiabatic and diabatic experimental data

The MIDA bank (Brega et al., 1990) also contains several sets of pressure drop data in adiabatic and diabatic conditions obtained with the same geometry. The latter data refer to situations in which starting from constant inlet conditions, the power is stepwise increased, in general up to the heat transfer crisis, but in a limited number of cases, also beyond it, up to the maximum permitted temperature of the test section. These data allow us to verify the coherence of the experimental data between adiabatic and diabatic conditions; this will be done by adopting the above described energy balance, *without using any empirical correlation.*

For this check, pressure drops in a heated duct are calculated as the integration of the adiabatic pressure drop trend along the heated length, and then compared to the actual diabatic experimental datum. The procedure is as follows:

1. Pairs (adiabatic–diabatic) of comparable sets (common geometry, same pressures and mass fluxes) are chosen.
2. For adiabatic and diabatic data, experimental friction pressure drops are derived by Eq. (22), where ρ_m is calculated as the average value between inlet and outlet conditions.
3. For adiabatic data, $(\Delta p/L)_{\exp}$ and $(\Delta p/L)_{f,\exp}$ are plotted versus the quality x.
4. Equivalent diabatic experiments with a given power and flow mass are chosen and for each one the quality x as a function of the generic channel position (l) and power is calculated, obtaining a linear trend (because the power is axially uniform)[1]:

[1] A very small departure from the linear law is due to the variation of the fluid enthalpies versus pressure along the duct.

Table 3
Comparison between friction pressure drops according to the two balances (Lombardi and Terlizzi, 1992).

$\left(\frac{\Delta p}{L}\right)_{exp}$ (kPa/m)	$\left(\frac{\Delta p}{L}\right)^{E}_{h}$ (kPa/m)	$\left(\frac{\Delta p}{L}\right)^{M}_{h}$ (kPa/m)	$\left(\frac{\Delta p}{L}\right)_{a,k}$ (kPa/m)	$\left(\frac{\Delta p}{L}\right)^{E}_{f,exp}$ (kPa/m)	$\left(\frac{\Delta p}{L}\right)^{M}_{f,exp}$ (kPa/m)	$\left(\frac{\Delta p}{L}\right)^{E}_{f,exp}/\left(\frac{\Delta p}{L}\right)^{M}_{f,exp}$
3.6289	0.7708	3.6256	0.0001	2.8600	0.0033	866
3.9090	0.5890	3.1400	0.0000	3.3200	0.7640	4.34
3.4400	1.4300	2.0690	0.0210	2.0100	1.3500	1.49

$$x = x(l) = \Delta x\left(\frac{l}{L}\right) + x_{in} \quad (24)$$

where Δx is obtained by an enthalpy balance between inlet and outlet, L is the overall length and x_{in} the inlet quality.

5. The diabatic total and friction pressure drops across the channel are then obtained solving the integral:

$$(\Delta p)^{\text{DIA}}_{\text{INT}} = \int_{\text{in}}^{\text{out}} \left(\frac{\Delta p}{L}\right)^{\text{ADIA}}_{\exp}(x)\,dl = \int_{x_{\text{in}}}^{x_{\text{out}}} \left(\frac{\Delta p}{L}\right)^{\text{ADIA}}_{\exp}(x)\,\frac{dx}{\Delta x} \quad (25)$$

where the subscript INT means *integrated* and $(\Delta p/L)^{\text{ADIA}}_{\exp}(x)$ is the total pressure drop in adiabatic conditions

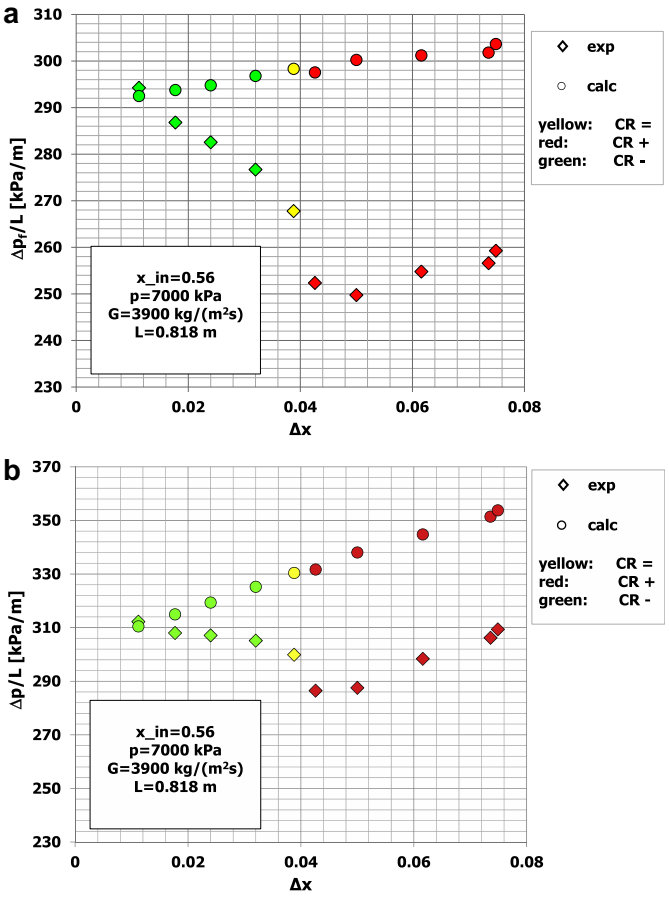

Fig. 2. a. Friction pressure drop against quality variation. Both experimental and calculated values are represented (MIDA bank Data sheet 8). b. Total pressure drop against quality variation. Both experimental and calculated values are represented (MIDA bank Data sheet 8).

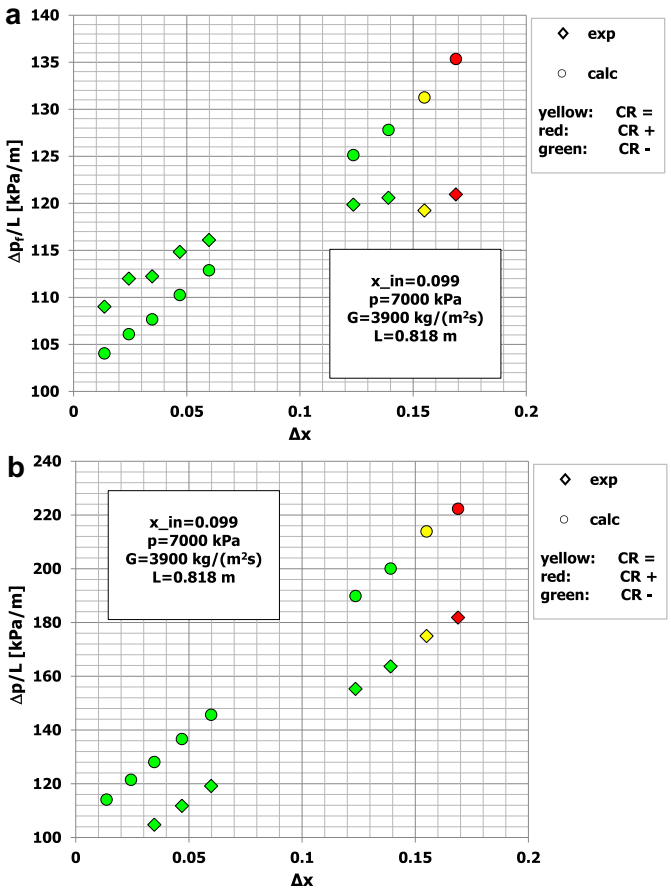

Fig. 3. a. Friction pressure drop against quality variation. Both experimental and calculated values are represented (MIDA bank Data sheet 8). b. Total pressure drop against quality variation. Both experimental and calculated values are represented (MIDA bank Data sheet 8).

6. The obtained values, divided by the length, and the corresponding experimental data of the pairs mentioned in 1) are as follows:

$$\left(\frac{\Delta p}{L}\right)^{DIA}_{f,exp} \text{ and } \left(\frac{\Delta p}{L}\right)^{DIA}_{f,INT}; \left(\frac{\Delta p}{L}\right)^{DIA}_{exp} \text{ and } \left(\frac{\Delta p}{L}\right)^{DIA}_{INT}$$

7. These data are compared for a certain number of similar conditions. In particular, some sets of data are chosen: those in which, starting from the same quality x_{in} (for a certain mass flux G_m and pressure) thermal crisis is reached and exceeded by increasing the power. Some examples are represented in Figs. 2a, 2b, 3a, 3b, and 4a, 4b, in terms of friction and total pressure drops respectively versus the quality increment along the duct, which is proportional to the power input; the points are differently coloured whether they are below, at and beyond the heat transfer crisis; the corresponding data are detailed in Tables 4–6. All sets of data, including those not here shown, present the same trend: an evident satisfactory agreement up to the thermal crisis, while beyond it there is an increasing difference, being the experimental value always lower than the integrated one. This behaviour is not unexpected, because in these conditions the wall liquid film is progressively destroyed along the duct, with a corresponding appreciable modification of the two phases flow distribution in the cross section, typical of adiabatic conditions. Preliminary CFD calculations, done by the authors, show that when the liquid film is broken or destroyed by the heat transfer crisis, the pressure drop trend is lowered with respect to the same hydrodynamic situation in adiabatic conditions.

Taking into account that conditions beyond thermal crisis are generally uncommon for power imposed systems (e.g. nuclear reactors or thermal boilers irradiated by a flame) or of limited length in imposed temperature systems (e.g. steam generators heated by a hotter fluid), it can be concluded that the application of the same empirical correlation to adiabatic and diabatic conditions is justified and numerically acceptable. In any case, the possible and limited overestimation of pressure drops is not a negative aspect for the design needs. This result is interesting because in spite of the fact that the kinetic term is increasingly important in diabatic conditions, the approximated homogeneous hypothesis for this term does not determine evident errors: it seems as though some compensation effect between friction and kinetic term takes place as power is added.

4. Revision of Cesnef-3 in the $Lo < k_2Ce$ zone

During the development of Cesnef correlations, the evidence that the linear relationship between the mixture friction *fm* and the dimensionless number *Lo* in logarithmic coordinates shows an abrupt change, has in our opinion a clear physical interest. We were

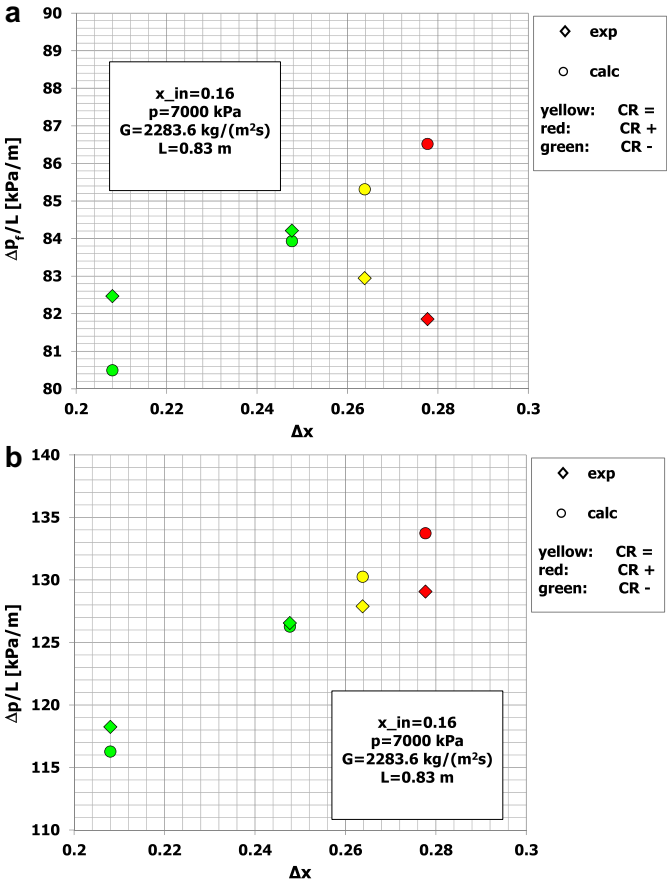

Fig. 4. a. Friction pressure drop against quality variation. Both experimental and calculated values are represented (MIDA bank Data sheet 17). b. Total pressure drop against quality variation. Both experimental and calculated values are represented. (MIDA bank Data sheet 17).

Table 4
Comparison between experimental diabatic and integrated adiabatic pressure drops.

	MIDA bank: Data sheet 8: $L = 0.818$ m; $G = 3900$ kg/m^2 s; $P = 7000$ kPa; $x_{in} = 0.56$								
	$N°$	Δx	$\Delta p/L$,exp (kPa/m)	$\Delta p/L$,int (kPa/m)	Δp_f,exp/L (kPa/m)	Δp_f,int/L (kPa/m)	Power (kW)	Error $\Delta P/L$ (%)	Error $\Delta P_f/L$ (%)
CR+	441	0.0736	306.20	351.42	256.59	301.81	8.17	−14.77	−17.63
CR+	443	0.0749	309.35	353.74	259.26	303.65	8.32	−14.35	−17.12
CR+	440	0.0616	298.37	344.78	254.79	301.19	6.79	−15.55	−18.21
CR+	438	0.0426	286.48	331.67	252.35	297.54	4.63	−15.77	−17.91
CR+	439	0.05	287.53	338.03	249.75	300.24	5.49	−17.56	−20.22
CR=	437	0.0388	299.87	330.40	267.78	298.31	4.19	−10.18	−11.40
CR−	434	0.0177	308.00	314.96	286.80	293.76	1.76	−2.26	2.43
CR−	435	0.024	307.10	319.34	282.55	294.80	2.49	−3.99	−4.33
CR−	433	0.0112	312.22	310.46	294.25	292.49	1.01	0.56	0.60
CR−	436	0.032	305.15	325.25	276.69	296.80	3.39	−6.59	−7.27

CR+ means above the thermal crisis; CR= thermal crisis; CR− below thermal crisis.

Table 5
Comparison between experimental diabatic and integrated adiabatic pressure drops.

	MIDA bank: data sheet 8: $L = 0.818$ m; $G = 3900$ kg/m^2 s; $P = 7000$ kPa; $x_{in} = 0.099$								
	$N°$	Δx	$\Delta p/L$,exp (kPa/m)	$\Delta p/L$,int (kPa/m)	Δp_f,exp/L (kPa/m)	Δp_f,int/L (kPa/m)	Power (kW)	Error $\Delta P/L$ (%)	Error $\Delta P_f/L$ (%)
CR+	389	0.1689	207.91	222.31	120.95	135.35	19.02	−6.93	−11.91
CR=	388	0.155	201.89	213.90	119.24	131.25	17.42	−5.95	−10.07
CR−	381	0.0598	148.90	145.68	116.10	112.88	6.51	2.16	2.77
CR−	380	0.0469	141.23	136.64	114.84	110.25	5.04	3.25	3.99
CR−	378	0.0244	127.38	121.47	112.00	106.08	2.47	4.64	5.28
CR−	377	0.0136	119.09	114.12	109.02	104.05	1.24	4.17	4.56
CR−	387	0.1391	192.85	200.07	120.59	127.81	15.61	−3.74	−5.99
CR−	386	0.1236	184.58	189.85	119.86	125.13	13.84	−2.86	−4.40
CR−	379	0.0347	132.64	128.07	112.24	107.67	3.64	3.45	4.07

CR+ means above the thermal crisis; CR= thermal crisis; CR− below thermal crisis.

facing a behaviour formally similar to that of single phase flow for the corresponding relationship between friction term and Reynolds number. While from a physical point of view, this latter change corresponds to the abrupt transition between laminar to turbulent flow, no physical explanation was found in two phase flow. To be concrete this change appears at very low flow rates and/or at high diameters, keeping constant the physical parameters (specific volumes, viscosities, and liquid surface tension). Then the idea to develop an improved correlation was that of trying to better define this transition point, by using a simpler correlation.

As said in section1, Cesnef-3 uses a different function for k_2, which makes this term rather complex and no longer dimensionless. The adoption of the ratio of the true liquid density over ambient water density is only a normalization process without any physical meaning.

In order to modify the following equation from Table 1:

$$k_2(\rho)Ce = \left[31,5\frac{\rho_l}{\rho_{l,0}} - 1,5\left(\frac{\rho_l}{\rho_{l,0}}\right)^2\right]\rho_l g\frac{(D-D_0)^2}{\sigma}\frac{\mu_g}{\mu_l} \tag{26}$$

the idea was to define a new dimensionless parameter *Ce*, which has been called *Cm* (*modified Cesnef number*):

$$Cm = \rho_l g\frac{(D-D_0)^2}{\sigma}\left(\frac{\mu_g}{\mu_l}\right)^n \tag{27}$$

where the suitable exponent n has to be found. Since transition in f_m versus *Lo* happens in correspondence of the value k_2 *Ce*, according to Cesnef-3 correlation, and the transition is at the same *Lo* number, it follows that at the *transition point*:

$$k_2(\rho)Ce = k_m Cm \tag{28}$$

or

$$k_2(\rho)\rho_l g\frac{(D-D_0)^2}{\sigma}\left(\frac{\mu_g}{\mu_l}\right) = k_m\rho_l g\frac{(D-D_0)^2}{\sigma}\left(\frac{\mu_g}{\mu_l}\right)^n \tag{29}$$

From this expression the value of a new parameter k_m can be obtained:

Table 6
Comparison between experimental diabatic and integrated adiabatic pressure drops.

	MIDA bank: data sheet 17: $L = 0.83$ m; $G = 2283.6$ kg/m^2 s; $P = 7000$ kPa; $x_{in} = 0.16$								
	$N°$	Δx	$\Delta p/L$,exp (kPa/m)	$\Delta p/L$,int (kPa/m)	Δp_f,exp/L (kPa/m)	Δp_f,int/L (kPa/m)	Power (kW)	Error $\Delta P/L$ (%)	Error $\Delta P_f/L$ (%)
CR+	208	0.2777	129.07	133.73	81.86	86.52	18.46	−3.61	−5.70
CR=	207	0.2638	127.89	130.25	82.95	85.31	17.53	−1.85	−2.85
CR−	206	0.2477	126.55	126.27	84.21	83.93	16.46	0.22	0.33
CR−	205	0.208	118.25	116.27	82.47	80.49	13.79	1.67	2.40

CR+ means above the thermal crisis; CR= thermal crisis; CR− below thermal crisis.

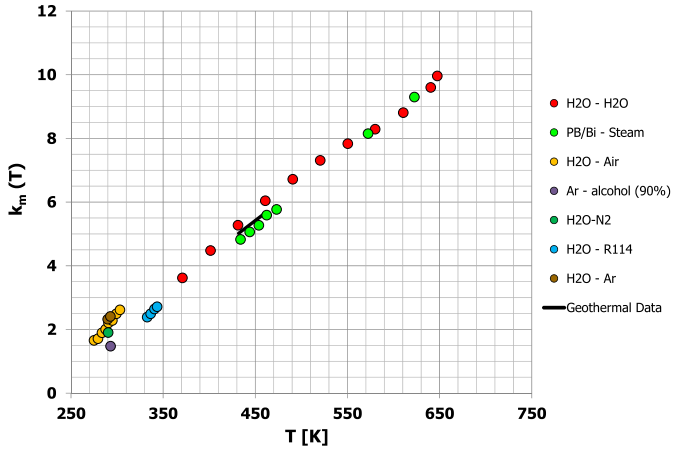

Fig. 5. k_m versus temperature.

$$k_m = k_2(\rho)\left(\frac{\mu_g}{\mu_l}\right)^{1-n} \tag{30}$$

Only a limited number of data in MIDA bank present this transition and referring to the liquid density and viscosities of the mixtures showing this trend, it was possible to calculate several values of k_m in function of n. Further k_m values are obtained by geothermal pressure drop data, which in three wells are always below this transition (Barelli et al., 1994).

After various attempts, it was arrived at the result that k_m may be a linear function of the temperature only, provided that n is equal to 1/3; then it is approximated by (see Fig. 5):

$$k_m = k_m(T) = 4.6\left(\frac{T}{T_0} - 1\right) \tag{31}$$

$T_0 = 207$ K where T is expressed in K.

Adopting this value, the Cesnef-3 correlation is modified in a new version named Cesnef 4, which is displayed in Table 7. By applying the correlation to all MIDA data having $Lo < k_m\,Cm$, the statistic of predictions confirmed the substantial coincidence with that obtained by Cesnef 3 (see Table 9). Moreover, by applying it to geothermal data the situation improved, with respect to the already satisfactory prediction by Cesnef-2, with an error reduction. The statistics is not here detailed because it requires a too wide presentation.

The objective of making the correlation, completely dimensionless, was not reached, but undoubtely the expression k_m is certainly simpler than $k_2(\rho)$ of Cesnef-3 and the predictions of geothermal data are improved. It was not possible to explain why the transition is dependent on temperature: this deserves a future investigation.

In conclusion, all this allows us to state that this correlation can substitute, with good reasons, the previous Cesnef 2 and Cesnef 3 ones.

5. Cesnef-4 versus experiments and other correlations

At the end of this work, a comparison is made, between Cesnef-4 and other three correlations, when used to predict experimental pressure drops. The data bank MIDA has been used. However, with respect to the comparison carried out in the past and summarized in Table 2, two choices have been made. First of all a certain number of data are not considered; they refer to rather exotic two phase mixtures, the phisical properties of which are difficult to find, as for instance a fluid made by a mixture of water and oil, or a mixture of water and alcohol, the data of which were badly predicted by Cesnef-2 and 3.[2] This reduces the number of available data from 16,154 to 10,996. The second choice is that of subdividing the data no longer by geometry, but by the type of mixture, because the designer in general is interested in the correlation reliability for the particular mixture considered in his application. Thirdly, the capillary data, which are few ones, are treated separately for all correlations, because their reliability is limited (the experimental procedure is really difficult and inherently approximate), so the predictions result rather poor in any correlation. Finally, the Pb–Bi/steam mixture are considered only for Cesnef 4 correlation, being the others not applicable in these mixtures.

The errors of the predictions are defined as:

- the average error (AE)

Table 7
Cesnef 4: Pressure drop correlation for two phase mixtures flowing in upflow in vertical ducts both in adiabatic and diabatic conditions.

The total pressure drop *dp* in an infinitesimal length *dh* is given by:
$dp = dp_f + dp_h + dp_k$
where:
$dp_f = \frac{2f}{D} G_m^2 v_m dh$ (friction term); $dp_h = \frac{1}{v_m} g dh$ (head term);
$dp_k = G_m^2 d v_m$ (kinetic term)
Note: when $Lo < k_m\,Cm$. dp cannot be higher than liquid column weight. i.e. $\rho_l\, g\, dh$.

Total friction factor
$f = f_g\, b_g + f_l\, b_l + f_m\, b_m$
f_g and f_l are single phase friction terms. calculated at the same total flow rate. and b_g. b_l and b_m are weight functions.

Single phase friction term
$f_{g/l} = \left[3.8 \log\left(\frac{10}{Re} + 0.2\frac{e}{D}\right)\right]^{-2}$ for $Re \geq 2400$
$f_{g/l} = \frac{16}{Re}$ for $Re < 2400$

Mixture friction term
$f_m = k_1\,(Lo)^{-0.25}$ for $Lo \geq k_m\,Cm$
$f_m = k_1(k_m\,Cm)\,Lo^{-1.25}$ for $Lo < k_m\,Cm$

Dimensionless numbers
$Lo = \frac{G_m^2 v_m D}{\sigma}\left(\frac{\mu_g}{\mu_l}\right)^{0.5}$
where $v_m = x\,v_g + (1-x)v_l$
$Cm = \rho_l g \frac{(D-D_0)^2}{\sigma}\left(\frac{\mu_g}{\mu_l}\right)^{1/3}$
where $D_0 = 0.001$ m
$C_m = 0$ when $D_0 \leq 0.001$

Constants
$k_1 = 0.044$; $k_m = 4.6\left(\frac{T}{T_0} - 1\right)$; $T_0 = 207$ K

Weight functions
$b_l = (1 - x_v)^{m_l}$; $b_g = x_v^{m_g}$; $b_m = 1 - b_g - b_l$
$m_{g/l} = \left[ln\left(e - 1 + \frac{v_g}{v_l}\right)\right]^{k_{gl}}$
$k_l = 0.5$; $k_g = 3.3$

Nomenclature
D = equivalent diameter; e = Neper number; G = mass flux; g = gravity; h = height; p = pressure; Re = Reynolds number; e = roughness; σ = surface tension; μ = viscosity; x = gas mass fraction; x_v = gas volumetric fraction
Subscripts: g = gas; l = liquid; m = mixture

[2] The researchers involved in these experiments told us that the alcohol-water mixture was transformed in a foam: this special mixture probably requires a specific approach (private communication).

Table 8
Error statistics for pressure drop predictions by four correlations.

Mixture		N°exp	D (m)	G (kg m^{-2} s^{-1})	p (kPa)	Cesnef-4		Friedel		Baroczy–Chisholm		MC Adams	
			min/max	min/max	min/max	AE %	RMS %	AE %	RMS %	AE %	RMS %	AE %	RMS %
H_2O/Ar		1323	7/25	50/3420	206/2237	−9.59	19.76	−22.24	42.16	3.66	38.65	−88.00	90.52
H_2O/H_2O+R114		707	446	112/2396	390/689	−0.23	4.48	−4.40	8.95	−4.32	8.91	−4.53	8.98
H_2O-Air		821	6/32	19/1570	99/343	−11.94	25.67	−27.52	48.31	13.78	26.68	−72.24	72.13
H_2O-N_2		434	25/105	20/3000	289/2383	−25.62	22.78	−36.44	49.75	−31.54	41.39	−58.80	82.66
H_2O-H_2O	A	2860	3/25	62/4577	72/9664	3.56	21.63	−7.79	19.95	6.71	24.40	−35.26	41.43
	D	4752	3/25	180/4072	121/8694	7.61	24.89	0.11	24.64	7.80	28.34	−20.03	32.40
ALL		10897	3/446	20/4577	72/9664	1.15	22.05	−8.50	27.30	5.10	27.70	−36.76	45.31
Cap		99	0.5/2.0	3.7/123	101	25.13	39.10	21.75	52.24	18.86	47.87	8.52	56.75

$$AE = \frac{1}{N}\sum_{i=1}^{N}\frac{\left(\Delta p_{calc} - \Delta p_{exp}\right)_i}{\left(\Delta p_{calc} \bullet \Delta p_{exp}\right)_i^{1/2}} \tag{32}$$

- the root mean square error (RMS)

$$RMS = \sum_{i=1}^{N}\left(\frac{AE_i^2}{N}\right)^{1/2} \quad \text{(Kotulski and Szczepinski, 2010)} \tag{33}$$

Between all available correlations for pressure drop in channels, three have been chosen mainly for two reasons: they are well known and widely used in thermo-hydraulics problems and easy to implement. Moreover, not all correlations found in literature are suitable for the range of data in MIDA bank. Then the correlations chosen, apart Cesnef-4, are:

- The Friedel correlation (Friedel, 1979);
- The Baroczy–Chisholm (Baroczy, 1966; Chisholm, 1973);
- The Mc Adams correlation (McAdams et al., 1942).

For cluster geometries, when present spacers the following equation is adopted:

$$\Delta p_{spac,TP} = \alpha K \frac{G_m^2}{2\rho_m} \tag{34}$$

Where K is the constant used in single phase flow (Idelchik, 2005) and α is a multiplier taken equal to 1.75 (Chiandet et al., 1991, suggests a value between 1.5 and 2).

The whole result is detailed in Table 8 and in Table 9 only for data in the $Lo < k_m\, Cm$. The following considerations can be done.

1. Cesnef-4 gives better predictions in both terms of AE and RMS for all mixtures;
2. Friedel and Baroczy–Chisholm correlations show a similar reliability, while Mc Adams gives unsatisfactory results, especially concerning two components mixtures.

For data in the $Lo < k_m\, Cm$ zone, the Cesnef 3 and 4 are almost equivalent, and this was expected, because the scope of Cesnef 4 is to simplify $k_m\, Cm$ without any quantitative variation; the other three correlations are worse, especially for two components mixtures.

6. Conclusions

Pressure drops in two phase flow is generally predicted by subdividing their value in three terms, in spite of the fact that in these conditions one of the terms, the empirically correlated friction one, is not independent from the duct inclination as in the single phase flow. However, following this procedure the energy balance is here preferred, instead of the momentum one, in order to avoid the exact prediction of the mixture density, by suitable correlations.

Since a number of pressure drops data of mixtures flowing upflow in vertical channels in adiabatic and diabatic conditions, are available by a specific data bank, it was possible to compare the corresponding behaviour, coming to the conclusion that it is almost the same, at least up to the heat transfer crisis of diabatic tests. By increasing the power beyond this one, the diabatic data show an increasing lower value, corresponding to the progressive destruction of the wall liquid film.

The Cesnef correlations (number 2 and 3) for predicting these pressure drops, as developed by our Department in the past, while yielding satisfactory predictions, have some drawbacks: fully dimensionless, but less general the first one and more general, but more complex and partially not dimensionless the second one. Then, the last one was simplified without obtaining a full dimensionless form and the resulting correlation is named Cesnef 4. A

Table 9
Error statistics for data in the region $Lo < k_m Cm$ by various correlations.

Mixture	N°exp	D (mm)	G (kg m^{-2} s^{-1})	p (kPa)	Cesnef-3		Cesnef-4		Friedel		Baroczy–Chisholm		MC Adams	
		min/max	min/max	min/max	AE %	RMS %	AE %	RMS %	AE %	RMS %	AE %	RMS %	AE %	RMS %
H_2O/Ar	14	6.93	50/200	1560	−10.17	19.26	−21.75	26.92	−74.81	79.08	−68.44	75.37	−92.72	99.68
H_2O/H_2O+R114	588	446	112/2396	364/628	−0.44	4.27	−0.19	4.08	−3.66	8.16	−3.59	8.13	−3.76	8.27
H_2O-Air	7	2.04	5.6/17	101	11.86	39.36	3.98	37.13	25.42	53.38	21.12	44.52	−6.51	39.45
H_2O-N_2	196	25/105	20/500	1167/2160	−26.23	43.32	−29.14	45.33	−64.75	89.85	−96.89	118.98	104.42	124.07
ALL	805	2/446	5.6/2396	101/2160	−6.78	14.35	−7.58	14.81	−19.52	29.68	−27.22	36.60	−29.84	38.32
Pb–Bi/steam	79	203/203	6211/14122	541/687	−6.40	6.87	−5.99	6.48	N.A	N.A	N.A	N.A	N.A	N.A

comparison with other three well known correlations by predicting about 11,000 data, confirms the better behaviour of Cesnef 4.

Nomenclature

Latin symbols

a	Coriolis coefficient
AE	average error
b	weight function
Ce	dimensionless number
Cm	dimensionless number
D	duct equivalent diameter
D_0	dimensional constant
e	specific kinetic energy; roughness
f	friction factor
G	mass flux
g	gravity acceleration
k_1, k_2, k_3, k_m	empirical constants
K	constant
Lo	dimensionless number
L	duct length
l	variable duct length
M	momentum
n	exponent
p	pressure
Re	Reynolds number
R_m	see Eq. (10)
T	absolute temperature
U	internal energy
u	velocity
v	specific volume
W_t	thermal energy
x	gas mass fraction
x_v	gas volumetric fraction
z	duct axis coordinate

Greek symbols

α	multiplier
β	see equation 21
γ	duct inclination
Γ	total mass flow rate
Δ	finite difference
μ	viscosity
ρ	density
σ	liquid surface tension
Ω	duct cross section area
τ	wall shear stress

Subscripts

a	acceleration
act	actual
$ADIA$	adiabatic
$calc$	calculated
DIA	diabatic
E	energy
exp	experimental
f	friction
g	gas
h	head
k	kinetic
in	inlet
INT	integral
l	liquid
m	mixture
M	momentum
out	outlet
$spac$	spacer

References

Barelli, A., Carsana, C.G., Lombardi, C.L., Maran, L., 1994. Prediction of geothermal well pressure and temperature profiles. Geothermics 23, 339–353.

Baroczy, C.J., 1966. A systematic correlation for two-phase pressure drop. Chem. Eng. Prog. Symp. Ser. 62, 232–249.

Bennett, C.O., Myers, J.E., 1974. Momentum, Heat and Mass Transfer, second ed. McGraw-Hill, NY, USA.

Brega, E., Brigoli, B., Carsana, C. G., Lombardi, C., Maran, L., 1990. MIDA: Data of Pressure and Densities Data of Two Phase Mixture Flowing in Rectilinear Ducts, 8th Congress UIT, Ancona, Italy, 1990.

Chiandet, R., Lombardi, C., Maran L., 1991. Spacer pressure drops in two-phase flow, 9th Congress UIT, Pisa, Italy.

Chisholm, D., 1973. Pressure drop due to friction during the flow of evaporating two-phase mixtures in smooth tubes and channels. Int. J. Heat Mass Transfer 16, 347–358.

Collier, J.G., Thome, J.R., 1996. Convective Boiling and Condensation. Oxford University Press, NY, USA.

Friedel, L., 1979. Improved friction pressure drop correlation for horizontal and vertical two-phase pipe flow. European two-phase flow group meeting, paper E2, Ispra, Italy.

Idelchik, I.E., 2005. Handbook of Hydraulic Resistance. Jaico Publishing House, Delhi, India.

Kotulski, Z., Szczepiński, W., 2010. Error Analysis with Applications in Engineering. Springer.

Lombardi, C., Carsana, G., 1992. A dimensionless pressure drop correlation for two phase mixtures flowing upflow in vertical ducts covering wide parameter ranges. Heat Technol. 10, 125–141.

Lombardi, C., Maran, L., Oriani, L., Ricotti, M.E., 2000. CESNEF-3 pressure drop correlation for gas-liquid mixtures flowing upflow in vertical ducts. 18th National Heat Transfer Conference, Cernobbio, Italy, June 28–30, 2000.

Lombardi, C., Terlizzi, A., 1992. Friction factor in upflowing two-phase mixtures according to energy or momentum balance, 29th meeting of the European two-phase flow group, Stockholm, June 1–3, 1992.

McAdams, W.H., Woods, W.K., Heroman, L.C., 1942. Vaporization inside horizontal tubes: II – benzene–oil mixtures. Trans. ASME 64, 193–200.